EFFECT OF CHORD LENGTH AND BOUNDARY CONDITIONS ON WELDS IN CHS X-JOINTS

KYLE TOUSIGNANT[1]

[1]*Department of Civil and Resource Engineering, Dalhousie University, 1360 Barrington Street, P.O. Box 15000, Halifax, Nova Scotia B3H 4R2, Canada.*
E-mail: kyle.tousignant@dal.ca

A finite-element (FE) investigation was conducted to determine the effect of chord length and boundary conditions (i.e. "end effects") on weld strength in circular hollow section (CHS) X-joints. One-hundred and fifty non-linear FE models of fillet-welded CHS X-joints, with variations in the chord length-to-radius ratio (α), brace-to-chord diameter ratio (β), chord slenderness ratio (2γ), and chord end boundary conditions were analyzed. All joints were modeled to be weld-critical (i.e. to fail by weld rupture) under quasi-static axial tension force(s) applied to the brace members via brace end displacements. Brace load vs. chord deformation behavior, weld rupture load, and strain adjacent to the weld were measured. By analysis of the results, it was found that "end effects" on weld strength in CHS X-joints are primarily a function of α, and are greatest for joints with high values of 2γ and β. A recent amendment to EN1993-1-8 that addresses minimum chord end distances to avoid adverse "end effects" (prEN1993-1-8 Clause 9.1.2(10)) based on joint tests is evaluated for welds designed as "fit for purpose".

Keywords: Circular hollow sections, X-joints, fillet welds, end effects, rigid cap plates.

1 Introduction

Over the last 30 years, research has been carried out to develop a "fit-for-purpose" design approach for welds in hollow structural section (HSS) joints. This approach permits sizing of welds to resist a force(s) in a brace, rather than to develop its capacity. Application of this "fit-for-purpose" approach relies on weld effective properties (e.g. weld effective lengths or section moduli) to account for the inherent non-uniform loading of the weld around an HSS joint caused by the non-uniform stiffness of the connected HSS wall. By using this approach to design welds (rather than designing them to develop the brace capacity), weld sizes and associated costs (e.g. joint preparation, material, and labor) can be substantially reduced.

Since the early 1990s, tests to determine weld effective properties have been carried out on rectangular hollow section (RHS) K-, X-, Y- and T-joints (Frater and Packer 1992a,b, Packer and Cassidy 1995, McFadden and Packer 2014, Tousignant and Packer 2015) and circular hollow section (CHS) X-joints (Tousignant and Packer 2017, 2018). However, these tests – and subsequent finite-element (FE) analyses (Tousignant and Packer 2018; Yaghoubshahi et al. 2019) – did not explicitly consider the effect of chord length and boundary conditions (i.e. "end effects") on weld strength.

Previous research has shown that the influence of "end effects" on joint strength can be significant (Bolt et al. 1992; Choo et al. 2006; van der Vegte and Makino 2006, 2010; Fan and Packer 2018). As a result, an amendment was recently made to EN 1993-1-8 (via prEN1993-1-8 Clause 9.1.2(10)) (CEN 2018) to give minimum end distances (e in Fig. 1) (and alternative

Proceedings of the 17th International Symposium on Tubular Structures.
Editors: X.D. Qian and Y.S. Choo

Published by Research Publishing, Singapore.
ISBN: 978-981-11-0745-0; doi:10.3850/978-981-11-0745-0_041-cd

requirements) for HSS joints. For CHS joints, prEN1993-1-8 Clause 9.1.2(10) (CEN 2018) is based on FE analyses of T- and X-joints (van der Vegte and Makino 2010) that were conducted to determine the influence of "end effects" on joint strength (i.e. the greater of: the peak brace load and the load at 3%d_0 chord deformation, where d_0 = chord diameter) (Fig. 1) (Lu et al. 1994). This paper presents a follow-up study to: (a) determine the influence of "end effects" on weld strength in CHS joints; and (b) evaluate prEN1993-1-8 Clause 9.1.2(10) (CEN 2018) for welds designed as "fit-for-purpose".

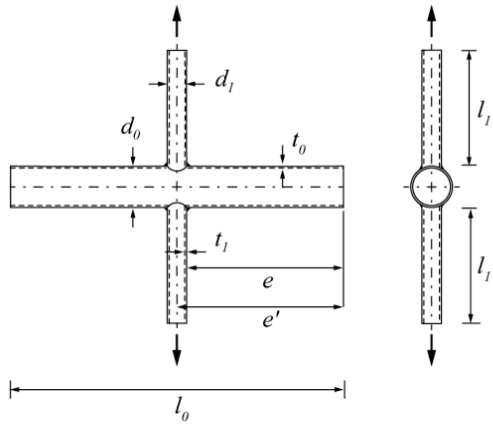

Figure 1. CHS X-joint terminology.

2 Finite Element Model Details

One-hundred and fifty FE models of CHS X-joints covering 14.0 ≤ chord slenderness ratio 2γ (= d_0/t_0, where t_0 = chord thickness) ≤ 63.5, 0.1 ≤ brace-to-chord diameter ratio β (= d_1/d_0, where d_1 = brace diameter) ≤ 0.5, and 8 ≤ chord length-to-radius ratio α (= $2l_0/d_0$, where l_0 = chord length) ≤ 24, with "rigid" or "free" chord ends, were analyzed (Table 1). All joints had brace-to-chord thickness ratio τ (= t_1/t_0, where t_1 = brace thickness) = 0.5, weld throat thickness $a = 0.5t_1$, brace-to-chord inclination angle $\theta_1 = 90°$, and brace length $l_1 = 3d_1$ (Fig. 1). The weld throat thickness ($a = 0.5t_1$) was selected so that weld fracture was the governing limit state.

The analyses were conducted using ANSYS 14.0 (Swanson Analysis Systems 2011) and one-eighth models of the X-joints (i.e. taking advantage of symmetry about three principal planes) (Fig. 2). All models (including the tensile coupons (TCs) discussed in Section 2.1) used eight-noded, SOLID45 finite elements (herein called the "typical elements") with reduced integration and hourglass control. The element and mesh details are summarized in Fig. 2.

Table 1. FE model geometric parameters.

		$\beta = d_1/d_0$		
		0.1	0.3	0.5
$2\gamma = d_0/t_0$	$d_0 \times t_0$ (mm × mm)	$d_1 \times t_1$ (mm × mm)		
14.0	406.4 × 29.0	40.6 × 14.5	121.9 × 14.5	203 × 14.5
25.6	406.4 × 15.9	40.6 × 7.9	121.9 × 7.9	203 × 7.9
36.9	406.4 × 11.0	40.6 × 5.5	121.9 × 5.5	203 × 5.5
50.8	406.4 × 8.0	40.6 × 4.0	121.9 × 4.0	203 × 4.0
63.5	406.4 × 6.4	40.6 × 3.2	121.9 × 3.2	203 × 3.2

Note 1: $\tau = 0.5$, $a = 0.5t_1$, $\theta_1 = 90°$, and $l_1 = 3d_1$ for all joints.
Note 2: Each of the 15 joints was analyzed with α = 8, 12, 16, 20, and 24, with rigid or free chord ends.

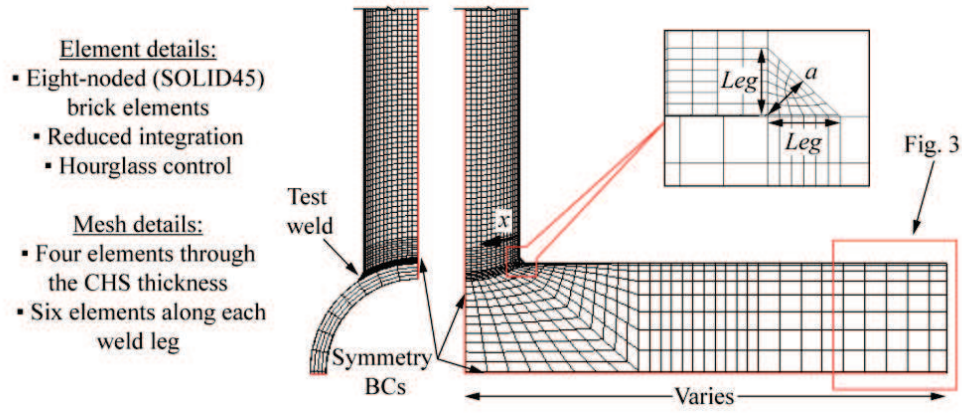

Figure 2. Typical CHS X-joint model; element and mesh details.

2.1 Material properties

The FE material properties were modeled on the results of TC tests conducted on CHS and filler metal materials in accordance with ASTM A370 (ASTM 2017) and AWS D1.1 (AWS 2015), respectively (Tousignant and Packer 2017). The CHS materials (for the braces and chord) were certified to ASTM A500 Grade B/C (with a minimum specified yield strength f_y = 317 MPa), and the filler metal (for the weld) was from an E71T-1C electrode (with a specified ultimate strength f_u = 490 MPa). The measured properties of these materials (f_y, f_u, and the Young's modulus E) are given in Table 2.

Table 2. Measured material properties (Tousignant and Packer 2017).

Material	f_y[1] (MPa)	f_u (MPa)	E (MPa)
CHS chord	460	540	208,000
CHS brace(s)	431	488	191,200
Filler metal	517	577	208,000

[1] f_y according to the 0.2% offset method (ASTM 2017).

These properties were modeled (for the "typical elements") in ANSYS using non-linear isotropic hardening, which relies on true stress-true strain (σ_t-ε_t) ordinate inputs to define material behaviour. Up to necking (i.e. when $\sigma \leq f_u$), the σ_t-ε_t ordinates were calculated from the engineering stress-engineering strain (σ-ε) ordinates (i.e. the results of the TC tests, for each different material) using Eqs. (1) and (2) (Boresi and Schmidt 2003):

$$\sigma_t = \sigma(1+\varepsilon) \tag{1}$$

$$\varepsilon_t = \ln(1+\varepsilon) \tag{2}$$

After necking (i.e. when $\sigma > f_u$), Eqs. (1) and (2) are no longer valid. The σ_t-ε_t ordinates were hence calculated using the hardening rule given by Eq. (3) (Ling 1996):

$$\sigma_t = \sigma_t' \left[w\left(1+\varepsilon_t-\varepsilon_t'\right)+\left(1-w\right)\frac{\varepsilon_t^{\varepsilon_t'}}{\varepsilon_t'^{\varepsilon_t'}} \right] \tag{3}$$

where σ_t' = true stress at start of necking; ε_t' = true strain at start of necking; and w = weighting factor.

In Eq. (3), the weighting factor w was calibrated (for each different material) by: selecting a trial value of w; computing the σ_t-ε_t ordinates after necking (using Eq. 3); modeling a TC in ANSYS (using the overall σ_t-ε_t curve, both before and after necking); generating a σ-ε curve for the TC using FE analysis; comparing that (FE) σ-ε curve the actual (experimental) σ-ε curve for the same TC; and iterating (as needed) until acceptable agreement was obtained. This "trial-and-error" approach for calibrating w in Eq. (3) is described in detail by Ling (1996).

2.1.1 Weld fracture modeling

Weld fracture (in the CHS X-joints) was simulated by using an equivalent strain "fracture criterion" (ε_{ef}) to trigger "element death" in ANSYS. When the equivalent strain $\varepsilon_e \geq \varepsilon_{ef}$, "element death" was initiated (for that element), reducing its stiffness (and equivalent stress) to near-zero. The affected element(s) hence freely deformed and shed its load to the surrounding elements (until $\varepsilon_e \geq \varepsilon_{ef}$ in those elements too, triggering their "death"). The analysis was run under quasi-static incremental displacements applied to the brace ends (in tension) until the brace tension load(s) stopped increasing (indicating that the ultimate load had been reached).

A value of $\varepsilon_{ef} = 0.32$ was previously calibrated by Tousignant and Packer (2018) for fracture occurring in fillet welds in CHS X-joints. That value ($\varepsilon_{ef} = 0.32$) was shown to minimize the error in actual-to-FE predicted fillet weld fracture/rupture load (P_u) for six tests on large-scale CHS X-joints with $\beta \leq 0.50$, $20 \leq 2\gamma \leq 34$, and $0.55 \leq \tau \leq 1.00$ (Tousignant and Packer 2017, 2018). The same value ($\varepsilon_{ef} = 0.32$) was used in the current study to initiate weld fracture. Only fracture in the welds (i.e. not in the base metal) was modeled.

2.2 *Chord end boundary conditions*

Seventy-five (out of 150) joints were modeled with "rigid" chord ends to evaluate the effect of a thick cap plate or a chord end connection (e.g. to another member) on weld strength. "Rigid" chord ends were modeled by adding a row of stiff ($E = 2\times10^9$ MPa), linear-elastic, SOLID45 elements (herein called the "stiff elements") to the end of the chord (Fig. 3a). The remaining 75 joints were modeled with "free" chord ends. "Free" chord ends were modeled without any special provisions, by using "typical elements" for the entire chord (Fig. 3b). As a result, "free" chord ends could deform (due to brace loads), and "fixed" chord ends could not.

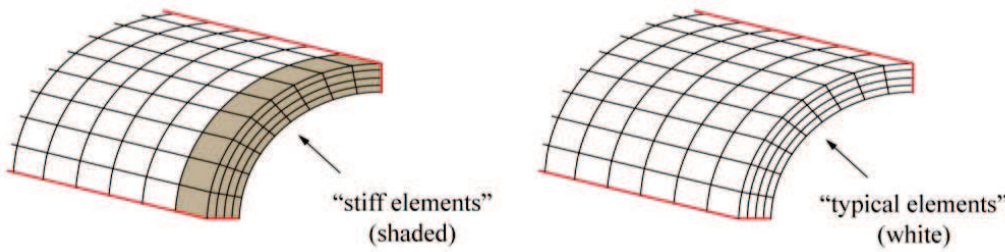

Figure 3. Chord end boundary conditions: (a) rigid chord ends; (b) free chord ends.

3 Finite Element Analysis Procedure and Results

As noted in Section 2.1.1, analyses were run under quasi-static incremental displacements applied to the brace ends. Displacements were applied in the theoretical "constant-stress region"

(at $l_1 = 3d_1$) (Mehrota and Govil 1972), and analyses included both material (Section 2.1) and geometric non-linearity. For each run, brace load (P), chord deformation (δ in Fig. 4a,b), P_u, and strain adjacent to the weld (in the brace, 25-mm from the connection) (ε) were output. Fig. 4a,b shows the results of normalized brace load (P/A_wf_u) vs. chord deformation (δ/d_0) behavior for a total of ten joints with "rigid" (Fig. 4a) and "free" (Fig. 4b) chord ends. Therein, f_u = ultimate strength of the filler metal (= 577 MPa in Table 2), $A_w = a \times l_w$, and l_w = total weld length (measured around the brace), and the influence of "end effects" on joint behavior (i.e. global stiffness and ultimate weld strength P_u/A_wf_u) can be seen.

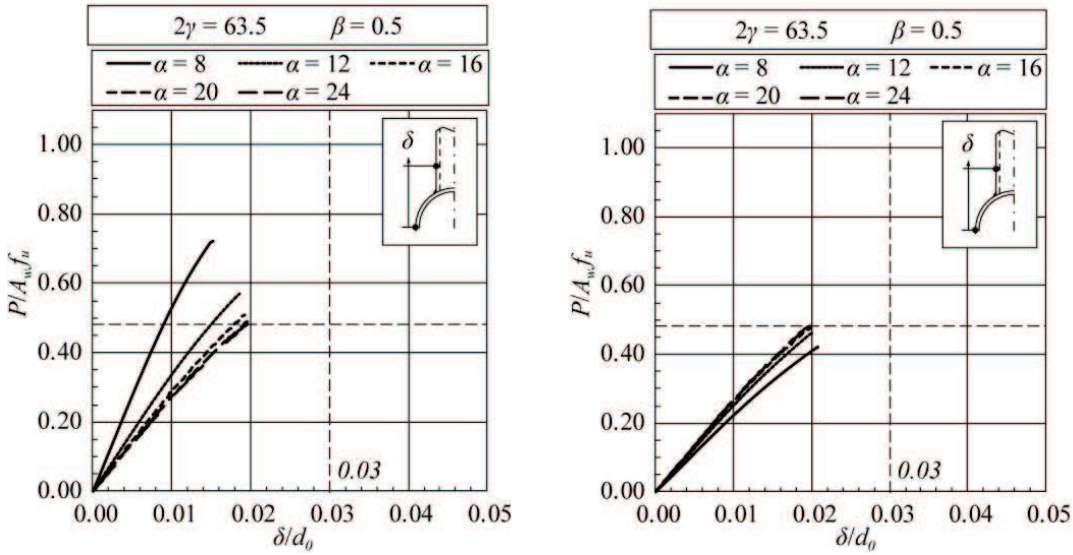

Figure 4. P/A_wf_u vs. δ/d_0 for joints with: (a) rigid chord ends; (b) free chord ends.

For 148 (out of 150) joints, P_u/A_wf_u occurred at $\delta < 3\%d_0$ (or $\delta/d_0 < 0.03$ in Fig. 4a,b) (Lu et al. 1994). Hence, nearly all of joints were "weld critical", meaning that weld rupture – not joint failure – was their governing limit state.

4 "End Effects" on Weld Strength

To evaluate "end effects" (on weld strength), P_u/A_wf_u is plotted against α (= $2l_0/d_0$) in Fig. 5a-d for 120 of the joints that were analyzed. In Fig. 5a-d, filled symbols denote joints with "rigid" chord ends and open symbols denote joints with "free" chord ends. For the joints shown (i.e. joints with $25.6 \le 2\gamma \le 63.5$), P_u/A_wf_u can be seen to vary predictably as a function of α: for joints with "fixed" chord ends, P_u/A_wf_u decreases as α increases, and for joints with "free" chord ends, P_u/A_wf_u increases as α increases. In both cases (i.e. "fixed" and "free" chord ends), "end effects" are greatest when β and 2γ are high. For joints that were analyzed but are not shown in Fig. 5a-d (i.e. joints with $2\gamma = 14.0$), P_u/A_wf_u was constant across all joints with the same value of β.

Fig. 6a,b shows typical plots of $\varepsilon/\varepsilon_{max}$ vs. x for selected joints with $2\gamma = 63.5$ and $\beta = 0.5$, where ε_{max} = maximum value of ε at a given brace load and x = "subtended angle" (i.e. the angle around the brace, measured from either crown point) (Fig. 2). Fig. 6a,b illustrates that the variations in P_u/A_wf_u depicted in Fig. 5a-d are due to changes in relative local stiffness (i.e. non-uniform load distribution) along the weld length.

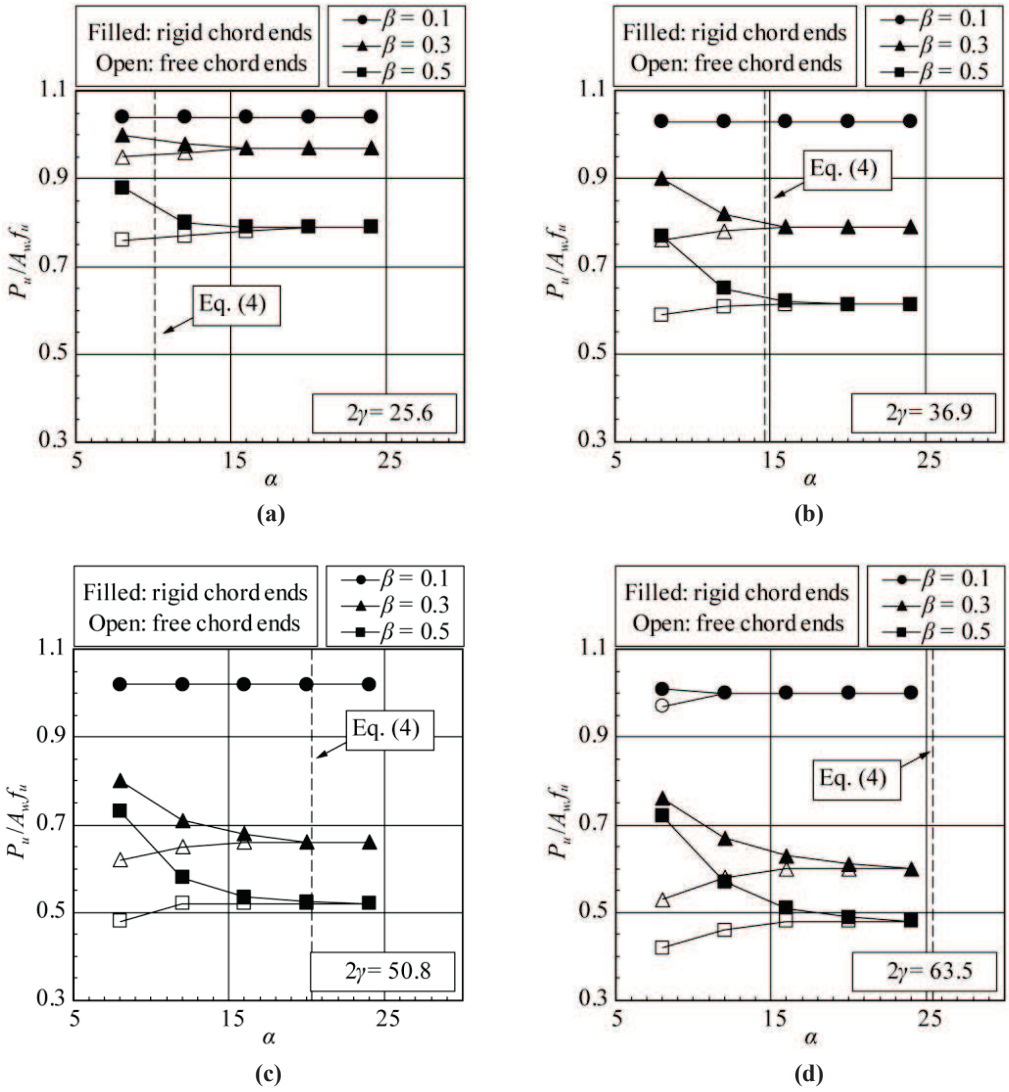

Figure 5. $P_u/A_w f_u$ vs. α for joints with: (a) $2\gamma = 25.6$; (b) $2\gamma = 36.9$; (c) $2\gamma = 50.8$; (d) $2\gamma = 63.5$.

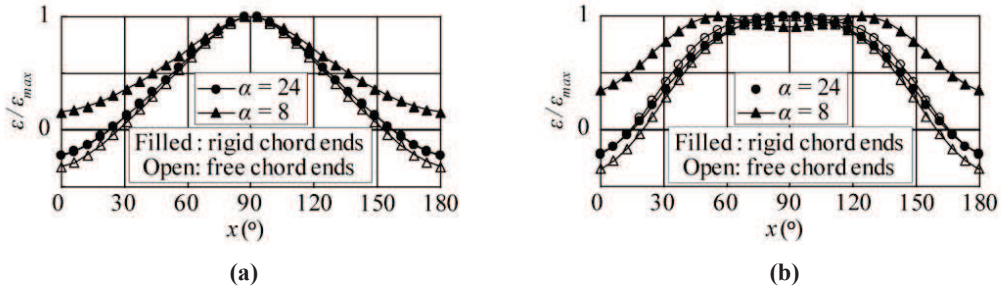

Figure 6. $\varepsilon/\varepsilon_{max}$ vs. x for joints with $2\gamma = 63.5$ and $\beta = 0.5$ at: (a) an initial elastic load; (b) rupture.

5 Evaluation of prEN1993-1-8 Clause 9.1.2(10)

Based on Section 4, it is therefore necessary to consider "end effects" when designing welds in CHS joints as "fit-for-purpose". Introduced in Section 1 of this paper, the following amendment (prEN1993-1-8 Clause 9.1.2(10)) (CEN 2018) was recently made to cover "end effects" for HSS joints (and presumably for welds) in EN1993-1-8:

> "for joints with a chord end not connected to other members, the chord end shall be at a distance of at least $(2\gamma/10)d_0$ from the heel or toe of the closest brace, with a minimum of $2.5d_0$…otherwise, the end shall be welded to a cap plate with a thickness of at least $1.5t_0$, at a minimum distance of $0.5d_0(1-\beta)$…from the brace toe or heel…"

For welds designed as "fit-for-purpose" (as permitted by EN1993-1-8 Clause 7.3.1(6)) (CEN 2010), validation of prEN1993-1-8 Clause 9.1.2(10) (CEN 2018) does not hitherto exist. To validate it using the current data, the minimum end distance (e in Fig. 1) given by prEN1993-1-8 Clause 9.1.2(10) (CEN 2018) as the maximum of $(2\gamma/10)d_0$ and $2.5d_0$ can conservatively be taken from the center of the joint (e' in Fig 1) (rather than from the heel or toe of the closest brace). It can then be shown that prEN1993-1-8 Clause 9.1.2(10) (CEN 2018) implies a minimum α (α_{min}) (to mitigate "end effects") of:

$$\alpha_{min} = \max\left(0.8\gamma,\ 10\right) \tag{4}$$

Eq. (4) is plotted in Fig. 5a-d as a vertical, dashed line (atop the current data). For joints with "free" chord ends (open symbols in Fig. 5a-d), $P_u/A_w f_u$ generally reaches a plateau while $\alpha \leq \alpha_{min}$. When this is not the case (e.g. when $2\gamma = 25.6$ in Fig. 5a), $P_u/A_w f_u$ when $\alpha > \alpha_{min}$ is at most 4% less than $P_u/A_w f_u$ for the same joint in the absence of "end effects". Considering that e (on which prEN1993-1-8 (CEN 2018) Clause 9.1.2(10) is based) is always be greater than e' (on which this evaluation is based), the reduction in $P_u/A_w f_u$ due to "end effects" in joints adhering to the minimum end distance in prEN1993-1-8 (CEN 2018) Clause 9.1.2(10) will be even less.

It can also be surmised (by looking at the joints with "rigid" chord ends in Fig. 5a-d) that the alternative requirements of prEN1993-1-8 Clause 9.1.2(10) (CEN 2018) (i.e. to connect the chord end(s) to another member or a rigid cap plate) will cause $P_u/A_w f_u$ to increase (relative to its value for the same joint in the absence of "end effects") when $\alpha \leq \alpha_{min}$. This can be deemed acceptable. The overall provisions of prEN1993-1-8 Clause 9.1.2(10) are hence sufficient to mitigate adverse "end effects" on welds in CHS joints designed as "fit for purpose" over the range of parameters studied.

6 Conclusions

Weld fracture was simulated in 150 FE models of fillet-welded CHS X-joints, with variations in α, β, 2γ, and chord end boundary conditions ("rigid" vs. "free") to determine the influence of "end effects" on weld strength in CHS joints. Based on the foregoing analysis, it was determined that:

(i) The weld strength ($P_u/A_w f_u$) varies predictably as a function of α;
(ii) when the chord ends are "rigid", $P_u/A_w f_u$ increases as α decreases;
(iii) when chord ends are "free", $P_u/A_w f_u$ decreases as α decreases; and
(iv) in both cases (i.e. "fixed" and "free" chord ends), "end effects" are greatest when β and 2γ are high.

These variations were shown to be due to changes in relative local stiffness (i.e. non-uniform load distribution) along the weld length (see Section 4).

The requirements of prEN1993-1-8 Clause 9.1.2(10), which give minimum end distances (e in Fig. 1) (and alternative requirements) for HSS joints were also evaluated. The overall provisions of this clause were found to be sufficient to mitigate adverse "end effects" on welds in CHS X-joints designed as "fit for purpose". The scope of these conclusions covers CHS joints with $14.0 \leq 2\gamma \leq 63.5$, $0.1 \leq \beta \leq 0.5$ and $\theta_1 = 90°$ that are symmetrical about the branch(es).

References

ASTM, *ASTM A370-17, Standard Test Methods and Definitions for Mechanical Testing of Steel Products*, ASTM International, West Conshohocken, PA, 2017.

AWS, *AWS D1.1/D1.1M:2015, Structural Welding Code – Steel,* American Welding Society, Miami, FL, 2015.

Bolt, H. M., Seyed-Kebari, H. and Ward, J. K., The Influence of Chord Length and Boundary Conditions on K-Joint Capacity, in *Proceedings of the 2nd International Offshore and Polar Engineering Conference*, 347-354, International Society of Offshore and Polar Engineers, San Francisco, CA, 1992.

Boresi, A. P. and Schmidt, R. J., *Advanced Mechanics of Materials, 6th ed.,* John Wiley and Sons, Inc., Hoboken, NJ, 2003.

CEN, *EN1993-1-8, Eurocode 3: Design of Steel Structures. Part 1-8: Design of Joints*, European Committee for Standardization, Brussels, 2010.

CEN, *prEN1993-1-8, Eurocode 3: Design of Steel Structures. Part 1-8: Design of Joints*, European Committee for Standardization, Brussels, 2018.

Choo, Y. S., Quian, X. D. and Wardenier, J., Effects of Boundary Conditions and Chord Stresses on Static Strength of Thick-Walled CHS K-Joints, *J. Constr. Steel Res.,* 62, 316-328, 2006.

Fan, Y. and Packer, J. A. RHS-to-RHS Axially Loaded X-Connections near an Open Chord End, *Can. J. Civ. Eng, CSCE,* 44, 881-892, 2017.

Frater, G. S. and Packer, J. A., Weldment Design for RHS Truss Connections, I: Applications. *J. Struct. Eng. ASCE*, 118(10), 2784-2803, 1992a.

Frater, G. S. and Packer, J. A., Weldment Design for RHS Truss Connections, II: Experimentation. *J. Struct. Eng. ASCE*, 118(10), 2804-2820, 1992b.

Ling, Y. Uniaxial True Stress-Strain after Necking, *AMP J. Technol.*, 5(1), 37-48, 1996.

Lu, L. H., de Winkel, G. D., Yu, Y., and Wardenier, J. Deformation Limit for the Ultimate Strength of Hollow Section Joints, in *Tubular Structure VI; Proc. Intern. Symp.*, Grundy, P., Holgate, A., Wong, B. (eds.), 341-348, Balkema, Netherlands, 1994.

McFadden, M. R. and Packer, J. A., Effective Weld Properties for Hollow Structural Section T-Connections under Branch In-Plate Bending, *Eng. J. AISC*, 51(4), 247-266, 2014.

Mehrota, B. L. and Govil, A. K., Shear Lag Analysis of Rectangular Full-Width Tube Connections, *J. Struct. Div, ASCE,* 98, 287-305, 1972.

Packer, J. A. and Cassidy, C. E., Effective Weld Length for HSS T, Y, and X Connections, *J. Struct. Eng., ASCE,* 121(10), 1402-1408, 1995.

Swanson Analysis Systems, ANSYS ver. 14.0. Houston, TX, 2011.

Tousignant, K. and Packer, J. A., Weld Effective Lengths for Rectangular HSS Overlapped K-Connections, *Eng. J. AISC.*, 52(4), 259-282, 2015.

Tousignant, K. and Packer, J. A., Fillet Weld Effective Lengths in CHS X-Connections I: Experimentation, *J. Constr. Steel Res.*, 138, 420-431, 2017.

Tousignant, K. and Packer, J. A., Fillet Weld Effective Lengths in CHS X-connections II: Finite Element Modelling, Parametric Study and Design, *J. Constr. Steel Res.*, 141, 77-90, 2018.

van der Vegte, G. J. and Makino, Y., Ultimate Strength Formulation for Axially Loaded CHS Uniplanar T-Joints, *Int. J. Offshore Polar, ISOPE, 1*6(4), 305-312, 2006.

van der Vegte, G. J. and Makino, Y., Further Research on Chord Length and Boundary Conditions of CHS T- and X-joints, *Adv. Steel Constr.,* 6(3), 879-890, 2010.

Yaghoubshahi, M., Sun, M. and Tousignant, K., Design of Fillet Welds in RHS-to-RHS Moment T-Connections under Branch in-plane Bending, *J. Const. Steel Res.*, 159, 122-133, 2019.